Femtosecond laser ablation of Au film around single pulse threshold

Xiaochang Ni (倪晓昌)[1,2], Ching-Yue Wang (王清月)[2], Yinzhong Wu (吴殷忠)[2], Li Yang (杨 丽)[2], Wei Jia (贾 威)[2], and Lu Chai (柴 路)[2]

[1]*Electronic Engineering Department, Tianjin University of Technology and Education, Tianjin 300222*

[2]*Key Laboratory of Optoelectronic Information Technical Science, EMC; Ultrafast Laser Laboratory, School of Precision Instruments and Optoelectronics Engineering, Tianjin University, Tianjin 300072*

Received July 6, 2005

Ablation process of 1-kHz femtosecond lasers (pulse duration of 148 fs, wavelength of 775 nm) of Au film on silica substrates is studied. The thresholds for single and multi pulses can be obtained directly from the relation between the squared diameter D^2 of the ablated craters and the laser fluence ϕ_0. From the plot of the accumulated laser fluence $N\phi_{\rm th}(N)$ and the number of laser pulses N, incubation coefficient of Au film is obtained to be 0.765. Some experimental data obtained around the single pulse threshold are in good agreement with the theoretical calculation.

OCIS codes: 140.3330, 160.3380, 310.3840, 260.3910.

There is increasing interest in the application of femtosecond laser pulses (10^{-15} s) in precision machining[1−4]. Many experimental results demonstrated that material processing with femtosecond laser possesses some unique advantages, such as absence of plasma shielding effect[2,3], well-defined ablation threshold, negligible heat-affected zone, no micro-cracks, and sub-wavelength features[4].

Femtosecond laser fabrication is associated with material and laser parameters. If the laser fluence applied to the sample exceeds a certain fluence $\phi_{\rm th}$ (material's fluence threshold), ablation occurs. The diameters of the ablated areas are influenced by the radius of the laser beam and can be used to characterize the ablation process, named incubation effect[5−8]. Most of studies on the incubation effect are concentrated on verifying the effect with dielectric materials rather than giving a guidance with other metal materials[8].

Figure 1 is the experimental setup of a commercial femtosecond laser (UMW-2110i, Clark-MXR Inc.) with a center wavelength of 775 nm, based on chirped pulse amplification (CPA) technique. The pulse duration measured by a scanning autocorrelator is 148 fs. The system provides variable output energies up to 1 mJ per pulse, which can be calculated from the average output power. A selected pulsed energy is realized through the attenuator after output mirror in CPA. And a desired pulse train can be obtained by the burst function of Pockels cell. The thermal incubation is very weak when the repetition rate is smaller than several GHz[9], therefore 1-kHz repetition rate is selected in this study. The target is mounted on a motorized x-y stage, whose resolution is 10 nm. A 5× objective is mounted on z stage during the experiment. All the processes can be controlled through the computer. And the ablated areas of the metal surface are characterized by an optical microscope (Hirox Inc., which can magnify target 3500 times) and scanning electron microscope (SEM). The film thickness is around 300 nm, which was deposited on silica substrates by sputtering method.

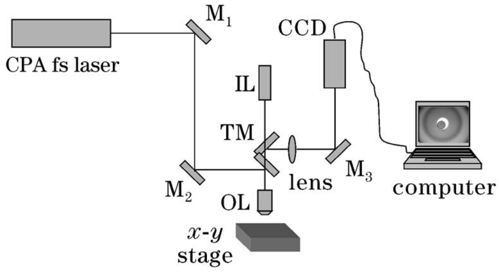

Fig. 1. Experimental setup of femtosecond laser micromachining. M_1—M_3: reflecting mirror; TM: part transmission and reflecting mirror; OL: objective lens; IL: illuminating laser.

In the case of a Gaussian spatial beam profile with a $1/e^2$-beam radius ω_0, the maximum laser fluence ϕ_0 in front of the surface depends linearly on the incident laser pulse energy $E_{\rm pulse}$[6]

$$\phi_0 = \frac{2E_{\rm pulse}}{\pi\omega_0^2}, \tag{1}$$

where ω_0 is 11.5 μm, which was measured by knife edge scan behind the objective[10].

The squared diameter D^2 of the ablated area and the laser fluence ϕ_0 at the sample surface satisfy[11]

$$D^2 = 2\omega_0^2 \ln\left(\frac{\phi_0}{\phi_{\rm th}}\right). \tag{2}$$

Figure 2 shows the ablated results for D^2 versus ϕ_0. The modification threshold $\phi_{\rm th}$ can be estimated by extrapolating the linear fit to $D^2 = 0$. The ablation thresholds are 0.656, 0.389, 0.301, and 0.220 J/cm^2 for single pulse, 5, 10, and 100 pulses respectively for Au film in air. The slopes ($2\omega_0^2$) of the linear fit lines are around 450 μm^2. So the experimental $1/e^2$-beam radius ω_0 can be obtained to be 15.0 μm close to the result of 11.5 μm with the knife scan method.

According to the incubation model[8], the relation between the multi pulse fluence threshold $\phi_{\rm th}(N)$ and the

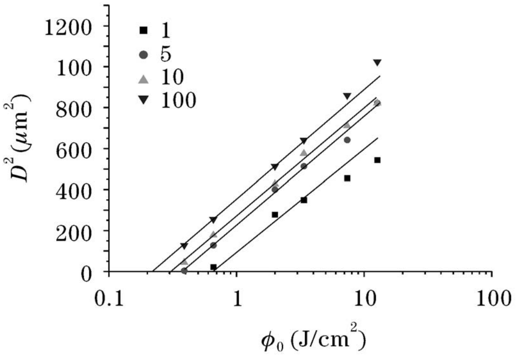

Fig. 2. The relation between squared diameters D^2 of the ablated areas and the applied laser fluence ϕ_0 for 1, 5, 10, 100 pulses processing of Au film in air. $\tau = 148$ fs, $\lambda = 775$ nm.

single pulse fluence threshold $\phi_{\rm th}(1)$ is given by

$$\phi_{\rm th}(N) = \phi_{\rm th}(1)N^{s-1}. \quad (3)$$

The exponent $s(< 1)$, incubation coefficient, characterizes the degree of incubation, which means that the ablation fluence threshold varies with the number of laser pulses N on the same spot.

To obtain s, Eq. (3) can be changed to

$$\log\left(N \cdot \phi_{\rm th}\left(N\right)\right) = \log\left(\phi_{\rm th}\left(1\right)\right) + s \cdot \log\left(N\right). \quad (4)$$

So depending on the results of Fig. 2, the relation of the accumulated laser fluence $N\phi_{\rm th}(N)$ at the ablation fluence threshold and the laser pulse N can be obtained in logarithmic coordinates, as shown in Fig. 3.

Figure 3 shows a good agreement of the experimental results with the incubation model. The value of $s = 0.765$ could be determined for femtosecond laser ablation of Au film in air.

However the value of s is lower than the previous research[11]. Different qualities of Au film may be the main reason. Here, the Au film used has been deposited half a year ago, which could be deliquesced during the summer. But the incubation coefficient s of material has been still successfully determined in the experiment.

Another important aspect of the laser processing is the determination of the ablation depth per pulse. There are two methods to determine the ablation rate. The

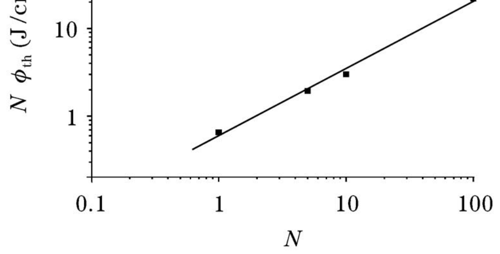

Fig. 3. Accumulated laser fulence $N\phi_{\rm th}(N)$ at the ablation threshold as a function of the number of laser pulses N for the ablation of Au film in air. The line represents a linear fit with a slope of $s = 0.765$ using Eq. (4).

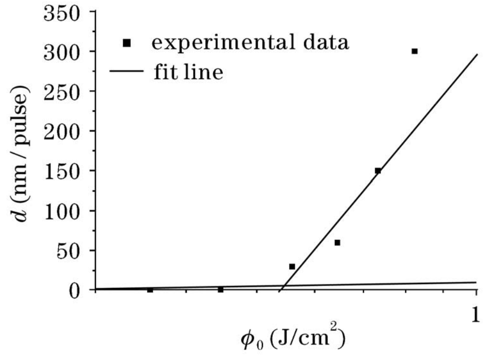

Fig. 4. The relation between ablation rate d and the femtosecond laser fulence of Au film in air, two regimes are used to fit experimental dots by $d \approx \alpha^{-1}\ln(\phi_0/\phi_{\rm th}^{\alpha})$, and $d \approx l\ln(\phi_0/\phi_{\rm th}^{l})$, respectively.

atomic force microscopy is used to judge the ablation depth with some laser pulses, and an average ablation depth per pulse can be obtained[12]. The other is the pump-probe method for the larger samples[13]. Here we characterize the ablation areas with Hirox microscope after laser exposure to judge whether the film is penetrated or not. If the film is just penetrated by a number of laser pulses ($N_{\rm threshold}$), the ablation rate d at the laser fluence can be obtained by $d = d_{\rm film}/N_{\rm threshold}$, where $d_{\rm film}$ is the thickness of Au film. To make the results very close to the true $N_{\rm threshold}$, the one pulse step is chosen around the pulse number with which the Au film is already penetrated. However for the case that laser fluence is very lower than that of single pulse threshold, incubation effect is so strong that it is not very obvious for small pulse step. So the larger pulse step is chosen in that case. Furthermore, when the laser fluence is lower than 0.20 J/cm^2, the ablation area cannot be found with the Hirox microscope in spite of how long the exposure time being extended. That is to say, the incubation effect has a fluence scale (lager than 0.20 J/cm^2 for Au film).

With this method, the laser fluence dependence of the ablation depth per pulse is given in Fig. 4. Figure 4 shows that ablation depth increases with the increase of the pulse energy and there are two ablation logarithmic regimes. This result coincides with previous research result obtained from a Cu thin film[14]. In the first regime, d is governed by the optical penetration depth α^{-1}, $d \approx \alpha^{-1}\ln\left(\phi_0/\phi_{\rm th}^{\alpha}\right)$, where $\phi_{\rm th}^{\alpha}$ is the fluence threshold of the first regime. In the second regime, the ablation depth d is determined by the heat diffusion length l, $d \approx l\ln(\phi_0/\phi_{\rm th}^{l})$, where $\phi_{\rm th}^{l}$ is the fluence threshold of the second ablation regime. Taking data from $\alpha^{-1} \approx 14.5$ nm[15] and $l = 1100$ nm[11], a logarithmic fit to the experimental data gives $\phi_{\rm th}^{\alpha} \approx 220$ mJ/cm^2 and $\phi_{\rm th}^{l} \approx 540$ mJ/cm^2.

This work was supported by the Key Grant Project of the Ministry of Education of China (No. 10410), the Science and Technology Development Project Fund of Tianjin (No. 043103911), the Specialized Research Fund for the Doctoral Program of Higher Education (No. 2003056021), and the Postdoctoral Science Foundation in China. X. Ni's e-mail address is xiaochang_ni@sina.com.

References

1. W. Chang, M. Choi, J. Kim, S. Cho, and K. Whang, Appl. Surf. Sci. **240,** 296 (2005).
2. X. Ni and C. Wang, Chin. J. Lasers (in Chinese) **31,** 277 (2004).
3. J. Liang, X. Ni, L. Yang, and Q. Wang, Chin. J. Lasers (in Chinese) **32,** 1291 (2004).
4. S. Bera, A. J. Sabbah, C. G. Durfee, and J. A. Squier, Opt. Lett. **30,** 373 (2005).
5. X. Ni, Q. Wang, Z. Wang, M. Hu, and Y. Li, Chin. Opt. Lett. **1,** 429 (2003).
6. J. Bonse, J. M. Wrobel, J. Krüger, and W. Kautek, Appl. Phys. A **72,** 89 (2001).
7. K. Ozono, M. Obara, A. Usui, and H. Sunakawa, Opt. Commun. **189,** 103 (2001).
8. P. T. Mannion, J. Magee, E. Coyne, G. M. O'Connor, and T. J. Glynn, Appl. Surf. Sci. **233,** 275 (2004).
9. X. Ni, Q. Wang, and J. Liang, Acta Photon. Sin. (in Chinese) **35,** 1 (2006).
10. J. Li, S. Cao, Z. Wu, Y. Wang, Z. Zhang, Y. Zhao, and X. Zhu, Nanotechnology and Precision Engineering (in Chinese) **3,** 142 (2005).
11. J. Güdde, J. Hohlfeld, J. G. Müller, and E. Mattias, Appl. Surf. Sci. **127-129,** 40 (1998).
12. J. Bonse, P. Rudolph, J. Krüger, and W. Kautek, Appl. Surf. Sci. **154-155,** 659 (2000).
13. X. Zhu, D. M. Villeneuve, A. Yu. Naumov, S. Nikumb, and P. B. Corkum, Appl. Surf. Sci. **152,** 138 (1999).
14. S. Nolte, C. Momma, H. Jacobs, A. Tünnermann, B. N. Chichkov, B. Wellegehausen, and H. Welling, J. Opt. Soc. Am. B **14,** 2716 (1997).
15. S. Preuss, A. Demchuk, and M. Stuke, Appl. Phys. A **61,** 33 (1995).